Instruction Material

Simulating quantum many-body dynamics on a current digital quantum computer

Day 2

Practical Training
Condensed Matter Theory
Technical University Munich
Physics Department

Responsible: Prof. Dr. Michael Knap

Available Dates (Day 1/Day 2):
January 21/22, 2021
May 20/21, 2021

1 Summary

In today's part of the training we apply the concepts introduced yesterday to a relevant many-body system using Google's Cirq library. The goal of this session is to study the phenomenon of Dynamical Quantum Phase Transitions (DQPTs) in a transverse field Ising model. Your task will be to convert the closed system quantum dynamics into a corresponding quantum circuit, and extract relevant observables such as the magnetization, the Loschmidt echo, and the entanglement dynamics from it. Along the way, we put an emphasis on the required measurement effort and the comparison with the exact solutions.

After the practical training day, please prepare a report in which you answer the questions posed throughout the instructions below, including a (brief) introduction to the topic. You can provide important plots in the main body of your report and attach the associated code in appropriately labelled appendices.

2 Prerequisites

1. Some minimal knowledge about quantum computation will be helpful, If you haven't learnt any quantum computation before, don't worry. A comprehensive reference will be the first chapter of *Quantum Computation and Quantum Information* by Nielsen and Chuang.

2. Before we start coding in Cirq, we will give instruction and some time for you to install Cirq. But if you can't wait, you can install the Cirq easily following the instruction here.

3. Please create a **Google account**, which is needed to work with Google Colab (a platform for interactive python notebooks). We provide a python notebook where you can find useful functions for completing the exercises.

4. The practical training consists of Day 1 (basics) and Day 2 (application), you are expected to hand in a written report for **both** Day 1 and Day 2, respectively. You can also choose to only participate on Day 1.

5. Please read through the following introduction on dynamical quantum phase transitions (section 3) and the transverse field Ising model (section 4) **ahead** of the practical session. You can follow the instructions even without answering the questions directly.

3 Dynamical Quantum Phase Transitions

In today's example we investigate the phenomenon of 'dynamical quantum phase transitions' (DQPTs). We provide a short introduction on the most important concepts based on the review of Ref [1]. DQPTs extend the notion of phase transitions

to the realm of non-equilibrium physics. Let us recall that for the more conventional equilibrium phase transitions, the central object is the partition function

$$Z = \mathrm{Tr}\; e^{-\beta \hat{H}(\alpha)}, \tag{3.1}$$

for an inverse temperature $\beta = 1/T$ and a Hamiltonian $\hat{H}(\alpha)$ that depends on a set of parameters α (e.g. the strength of an external magnetic field). The partition function Z provides an implicit definition of a free energy density $f(\beta, \alpha)$ via

$$Z = e^{-\beta N f(\beta,\alpha)}, \tag{3.2}$$

which depends on both β and the collection of parameters α. N denotes the size of the system. Equilibrium phase transitions then occur at points where the free energy density $f(\beta, \alpha)$ becomes *non-analytic* as a function of either β or one of the parameters α. The former are temperature-driven phase transitions at some critical temperature T_c. The latter, if occuring at zero-temperature, are called quantum phase transitions.

In the context of DQPTs we now instead consider the real time evolution of a closed quantum many-body system starting from the ground state $|\psi_0\rangle$ of some Hamiltonian $\hat{H}_0$. At time $t = 0$, the Hamiltonian is abruptly changed from $\hat{H}_0$ to $\hat{H}$, a protocol which is called a *quantum quench*. Formally, the time evolution is then solved by

$$|\psi_0(t)\rangle = e^{-i\hat{H}t}\; |\psi_0\rangle\,. \tag{3.3}$$

A formal similarity to the above partition functions is achieved by computing the return amplitude to the original ground state $|\psi_0\rangle$,

$$\mathcal{G}(t) = \langle\psi_0|\psi_0(t)\rangle = \langle\psi_0|e^{-i\hat{H}t}|\psi_0\rangle\,, \tag{3.4}$$

which is called the *Loschmidt amplitude*. The associated return probability

$$\mathcal{L}(t) = |\mathcal{G}(t)|^2 = \left|\langle\psi_0|\psi_0(t)\rangle\right|^2 \tag{3.5}$$

is usually referred to as the *Loschmidt echo*. In analogy to the above equilibrium partition functions, the Loschmidt amplitude takes on a particular dependence on system size N (for large values N), such that we can write

$$\mathcal{G}(t) = e^{-N\, g(t)}, \tag{3.6}$$

with an associated (complex) rate function $g(t)$. Similarly, the Loschmidt echo is written as

$$\mathcal{L} = e^{-N\, \lambda(t)}. \tag{3.7}$$

We will refer to the rate function $\lambda(t)$, which can alternatively be defined as $\lambda(t) = -\lim_{N\to\infty} \frac{1}{N} \log \mathcal{L}(t)$ in the thermodynamic limit, as the *Loschmidt rate*.

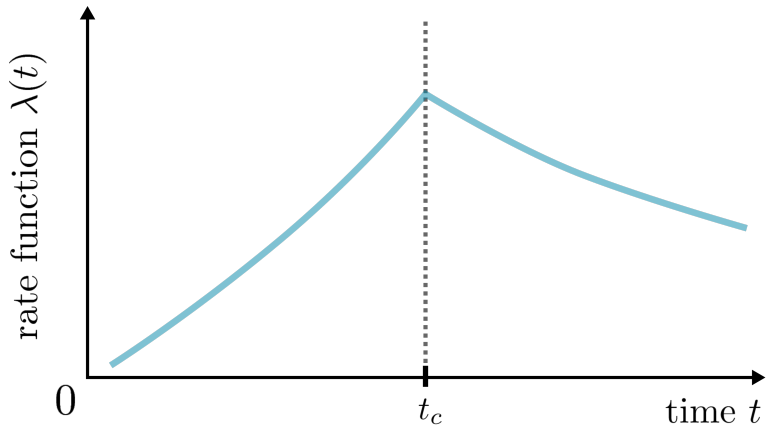

Figure 1: ***Dynamical Phase Transition.*** *(Figure 1 from Ref. [1]) At critical times t_c, the Loschmidt rate $\lambda(t)$ experiences non-analytic kinks.*

> ***Exercise 1:*** Show that $\lambda(t)$ and $g(t)$ are related via $\lambda(t) = 2\,\mathrm{Re}[g(t)]$. The exponential dependence of $\mathcal{G}(t)$ and $\mathcal{L}(t)$ on system size N in Eq. (3.6) and Eq. (3.7) is only in general valid if the quench changes the energy density, i.e. inserts an extensive amount of energy into the system. Can you come up with an intuitive reason for this (no calculations necessary)?

Equipped with these definitions, we can now identify DQPTs as points where the rates $\lambda(t)$, $g(t)$ become non-analytic as a function of time. DQPTs occur at *critical times* t_c where the rate $\lambda(t_c)$ typically shows a kink-like behavior in the thermodynamic limit, see Fig. 1 for a sketch.

> *Technical Note:* The analogy between partition functions and the Loschmidt amplitude can be made more concrete by interpreting
>
> $$\mathcal{G}(z) = \langle\psi_0|e^{-i\hat{H}z}|\psi_0\rangle\,, \qquad z \in \mathbb{C}, \tag{3.8}$$
>
> as a so-called 'boundary partition function' for a general complex parameter z. Non-analyticities of the associated rate function $g(z)$ are then associated to the zeros of $\mathcal{G}(z)$ in the complex plane (called Fisher zeros). A DQPT occurs whenever such Fisher zeros intersect the real axis, see Ref. [1] for more information.

As a final definition for this section, we note that one can generalize the Loschmidt echo $\mathcal{L}(t)$ for situations where the initial Hamiltonian $\hat{H}_0$ has more than one ground state, i.e. in the presence of spontaneous symmetry breaking: If $|\psi_i\rangle$ with $i = 0, ..., N_{gs} - 1$ labels all the N_{gs} states in the ground state manifold of $\hat{H}_0$, the

Loschmidt echo becomes

$$\mathcal{L}(t) = \sum_{i=0}^{N_{gs}-1} \left|\langle\psi_i|\psi_0(t)\rangle\right|^2, \tag{3.9}$$

and can be interpreted as the return probability to the ground state manifold of $\hat{H}_0$. In addition to the usual Loschmidt rate $\lambda(t) = -\lim_{N\to\infty} \frac{1}{N} \log \mathcal{L}(t)$, we can then also define the individual rates $\lambda_i(t)$ via

$$\left|\langle\psi_i|\psi_0(t)\rangle\right|^2 = e^{-N\lambda_i(t)}. \tag{3.10}$$

Exercise 2: Based on the above definitions, show that in the thermodynamic limit $N \to \infty$, the Loschmidt rate $\lambda(t)$ reduces to the minimum function applied to the set of individual rates $\lambda_i(t)$, i.e. $\lambda(t) = \min_i [\lambda_i(t)]$.

4 The transverse field Ising model

We now consider a specific example to study DQPTs in the following , the paradigmatic transverse field Ising model (TFI). It is a ubiquitous model in the field of many-body physics and, due to its exact solvability, often used to benchmark numerical methods, including quantum computers.
In one dimension, the TFI consists of a linear chain of N qubits (or spin-1/2 sites) whose time evolution is generated by the following Hamiltonian,

$$\hat{H} = -\frac{1}{2}\sum_{\langle i,j\rangle} Z_i Z_j - \frac{g}{2}\sum_i X_i, \tag{4.1}$$

where $\langle i, j\rangle$ denotes nearest neighbor sites. We set the strength of the ZZ - Ising interaction to unity, but vary the strength g of the transverse field. The computational basis can be chosen as the z-basis in the following.
Before delving into the implementation as a quantum circuit, let us first perform a proper analysis of the model's symmetries and zero temperature (i.e. ground state) phase diagram.

Exercise 3: Show that the parity operator

$$\hat{P} = \prod_i X_i \tag{4.2}$$

commutes with the Hamiltonian, i.e. $[\hat{H}, \hat{P}] = 0$. What is the spectrum of $\hat{P}$, i.e. its possible eigenvalues? Determine the exact ground states of $\hat{H}$ in the two limiting cases $g = 0$ and $g \to \infty$. Notice that for

$g = 0$, the symmetry $\hat{P}$ is spontaneously broken, i.e. an infinitesimally small longitudinal field $\pm\epsilon \sum_i Z_i$ induces a finite expectation value of the ground state magnetization $m_z = \frac{1}{N}\sum_i Z_i$. Compute the expectation value of m_z in the respective symmetry broken ground states at $g = 0$, as well as for the ground state at $g \to \infty$.

From the solution to Exercise 3 we see that the TFI features a symmetry-broken ferromagnetic phase, i.e. $m_z(g) \neq 0$, for $g < g_c$ smaller than some so far unknown critical field strength g_c. As mentioned above, the TFI can be solved exactly and $m_z(g)$ can be computed analytically [2]. However, for our purposes, there is a more direct way to infer the critical field g_c:

Exercise 4: Let us introduce the new Ising variables $\tilde{Z}_n = \prod_{i \leq n} X_i$ and $\tilde{X}_n = Z_n Z_{n+1}$, that can be thought of as living on the bonds of the lattice. Show that indeed $\{\tilde{Z}_n, \tilde{X}_n\} = 0$ as required, and express the Hamiltonian in terms of these new variables. Compare the result with the form of the Hamiltonian in terms of the original variables X_i, Z_i. How can you conclude from the resulting self-dual structure that the critical field assumes the value $g_c = 1$? The above transformation is known as the Kramers-Wannier duality transformation.

The previous analysis sets the stage for the investigation of DQPTs in the TFI model. In particular, we now know that for $g < 1$, the ground state manifold contains two degenerate ferromagnetic states $|\psi_0\rangle$ and $|\psi_1\rangle$ which are related by flipping all spins, $|\psi_1\rangle = \hat{P}\,|\psi_0\rangle$. For $g > 1$ the unique ground state is a paramagnet. Before shifting to numerics, let us answer the following final question:

Exercise 5: We have shown the presence of ferromagnetic order in the ground state for $g < 1$. Does this order survive at finite temperatures? *Hint:* How much energy does a domain wall between two ferromagnetic patches cost? Accordingly, how many domain walls as a function of system size do you expect at finite temperatures? Use your result to argue that there can be no long-range ferromagnetic order at finite temperatures.

5 DQPTs in the TFI using Cirq

We now turn to the simulation of the time evolution generated by $\hat{H}$ using the methods introduced on Day 1 of the practical. In addition to this manual, your instructors will provide you with a python notebook containing several pre-defined functions that you may use to perform the following tasks.

5.1 Implementing the time evolution

Given $\hat{H}$ from Eq. (4.1), we want to perform a Trotter decomposition of the unitary operator $U(t) = e^{-i\hat{H}t}$, based on the elementary exponentials $e^{-iZ_iZ_j\,dt}$ and $e^{-igX_i\,dt}$ that can directly be implemented in Cirq. To this end, we can rewrite

$$U(t) = e^{-i\hat{H}t} = \left(e^{-i\hat{H}\,dt}\right)^{t/dt} = \left(e^{\hat{A}+\hat{B}}\right)^{t/dt}, \tag{5.1}$$

with $\hat{A} = -\frac{g}{2}dt\sum_i X_i$ and $\hat{B} = -\frac{1}{2}dt\sum_{\langle i,j\rangle} Z_iZ_j$.

Exercise 6: Based on the functions expZZ(t) and expX(t) provided in the python notebook, define
a) A function evolve_basic(circ,qubits,g,dt) that takes the input circuit circ and appends a set of operations that evolve the system of qubits by a small time step dt based on the first order Trotterization $e^{\hat{A}+\hat{B}} \approx e^Ae^B$.
b) A function evolve_symmetric(circ,qubits,g,dt) that takes the circuit circ and appends a set of operations that evolve the system by dt based on the second order Trotterization $e^{\hat{A}+\hat{B}} \approx e^{A/2}e^Be^{A/2}$.

In both cases, for the nearest neighbor Ising interaction you can approximate

$$e^{-i\delta t\sum_{\langle i,j\rangle} Z_iZ_j} \approx \prod_{i=0}^{N/2-1} e^{-i\delta t\,Z_{2i}Z_{2i+1}} \prod_{i=0}^{N/2-2} e^{-i\delta t\,Z_{2i+1}Z_{2i+2}}. \tag{5.2}$$

Exercise 7: To benchmark the results from Exercise 6, simulate the time evolution and extract the magnetization $m_z(t)$ as a function of time for a system of $L = 10$ qubits at $g = 2$, starting from an initial state $|\psi_0\rangle = |0...0\rangle$ of all spins down. Compare your results to the magnetization obtained through exact diagonalization of the Hamiltonian, which is provided by the pre-defined function magn_exact_diagonalization(L,g,t,dt) in the python notebook. How small do you have to choose the time step dt in the circuit to obtain a good approximation to the exact results for a final time of $t = 5$?

5.2 Extracting DQPTs

We now want to evaluate the Loschmidt rate as described at the beginning of this manual. The initial Hamiltonian is chosen as $\hat{H}|_{g=0}$, where the two degenerate ferromagnetic ground states are $|\psi_0\rangle = |0...0\rangle$ and $|\psi_1\rangle = |1...1\rangle$.

Exercise 8: Using the same time evolution as above, extract the simulated Loschmidt rate by projecting back onto the ground state manifold, see Eq. 3.9. Plot $\lambda(t)$, as well as the individual rates $\lambda_{1/2}(t)$, for
a) Different system sizes $L = 6, 8, 10, 12$ and $g = 2.0$. Can you see DQPTs emerging?
b) Different values of g between $0.5 \leq g \leq 1.5$. For which of these values are there DQPTs and for which not?

In the actual quantum device, we do not have access to the simulated wavefunction directly, and have to determine observables by repeated measurements.

Exercise 9: Determine both the magnetization and Loschmidt echo again, this time via repeated measurements. Plot your results for $L = 10$ and $g = 2.0$. How much sampling (as a function of system size) is in principle necessary to obtain accurate results?

Exercise 10: Compare the time evolution of the magnetization $m_z(t)$ with the Loschmidt rate $\lambda(t)$ (you may put both quantities into the same plot). Can you see any correspondence between $m_z(t)$ and $\lambda(t)$?

5.3 Tracking the entanglement production I: State Tomography

During the time evolution following the quantum quench, the system builds up entanglement. The increase in entanglement is responsible for the limitations on using classically efficient methods (e.g. matrix product states) to simulate the dynamics up to arbitrary times. To quantify the amount of entanglement in the system we consider the half-chain entanglement von Neumann entropy as well as the second Rényi entropy. For this purpose, we first define the reduced density matrix ρ_ℓ of the left half of the system,

$$\rho_\ell = \mathrm{Tr}_r\,[\rho], \tag{5.3}$$

with ρ the density matrix of the full system. The von Neumann entanglement entropy S is then defined as

$$S = -\mathrm{Tr}[\rho_\ell \log(\rho_\ell)]. \tag{5.4}$$

The second Rényi entropy on the other hand is obtained from ρ_ℓ via

$$S^{(2)} = -\log(\mathrm{Tr}[\rho_\ell^2]). \tag{5.5}$$

Exercise 11: We first extract the entanglement from the simulated wave function of the quantum circuit. Do so in the following way:
a) Define two functions vN_entropy(rho) and renyi2_entropy(rho) that return S and $S^{(2)}$ from Eqs. (5.4) and (5.5) for a given density matrix ρ, respectively. *Hint:* In order to compute S, express the trace in Eq. (5.4) in the eigenbasis of ρ.
b) Use the functions from part a) to compute and plot both $S(t)$ and $S^{(2)}(t)$ as a function of time for $g = 2$ (again starting from the ferromagnetic initial state $|\psi_0\rangle = |0...0\rangle$). Verify that both $S(t)$ and $S^{(2)}(t)$ grow *linearly* in time.

In order to obtain the reduced density matrix from the measured data, one needs to use state tomography. The principle of state tomography is readily explained (following Ref. [3]): Consider a single qubit (compare also with Day 1 of the practical), whose state is described by a point on (or within for mixed states) the Bloch sphere, i.e. three independent coordinates. Measuring the state of the qubit in the computational z–basis yields the z–component $\langle z\rangle = p_o - p_1$ on the Bloch sphere. In order to determine the y–component, we simply rotate around the x–axis by $\pi/2$ before measuring, in order to bring the y–axis upright. Analogously, rotation around the y–axis by $-\pi/2$ brings the x–axis upright and allows to determine the x–component.
For a system of N qubits with density matrix ρ, the above Ansatz is straightforwardly generalized: We apply all 3^N possible combinations of rotations of the individual qubits before measuring, denoted by U_j with $j \in \{1, ..., 3^N\}$. For a given rotation U_j, we then measure the probabilities p_{jk} of all basis states $|k\rangle$, with $k = 1, ..., 2^N$. This can be expressed as

$$p_{jk} = \langle k| U_j^\dagger \, \rho \, U_j \, |k\rangle \, . \tag{5.6}$$

Using the measured probabilities p_{jk} as inputs, Eq. (5.6) can straightforwardly be solved for the density matrix ρ by linear inversion. Notice however, that due to the limited amount of measurements, the resulting ρ is not guaranteed to be physical. Therefore, the ρ extracted from the measurements has to be be post-processed in order to find the physical density matrix that provides the best fit to the measured ρ. In the python notebook, we provide the function MLE_minimal(rho) that performs this task.

Exercise 12: For $L = 10$ and $g = 2$, perform a state tomography experiment with tomo_rep $= 2000$ repeated measurements (you can try out smaller numbers first) for each basis rotation. From the resulting probabilities p_{jk}, extract the associated density matrix and feed it into the provided function MLE_minimal(rho) in order to obtain the physical density matrix that best describes your measurement outcomes. Extract the corresponding von Neumann and second Rényi entropies as a function of time and compare them to the above exact results.

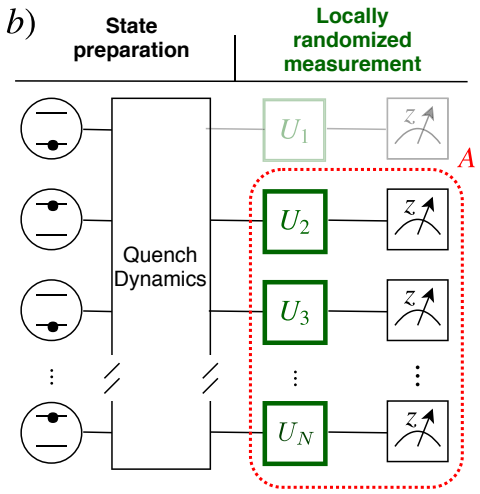

Figure 2: ***Randomized Measurements*** *(Figure 1b from Ref. [5]) Before measuring the qubits of subsystem A, random unitaries U_i are applied to the individual qubits. Correlations between these randomized measurement outcomes yields the second Rényi entropy according to Eq. (5.8).*

> ***Exercise 13:*** *(optional)* If you are interested, it is instructive to read through Ref. [4] (accessible at https://arxiv.org/abs/1106.5458) to see how the algorithm used in the function MLE_minimal(rho) works.

5.4 Tracking the entanglement production II: Randomized Measurements

Above, we extracted the von Neumann and second Rényi entanglement entropies through state tomography. However, for the second Rényi entropy (as well as for even higher Rényi entropies), there is a less costly way to extract $S^{(2)}(t)$ via *randomized measurements*. In this procedure, following Ref. [5], before the qubits are measured, we apply a random unitary operation $U = \prod_i U_i$ (with $i = 1, ..., L$) to each individual qubit of the chain, see Fig. 2, and use the statistical correlations between such randomized measurements in order to determine $S^{(2)}(t)$.

Let us go through the individual steps of this scheme more specifically:
1) Each U_i is chosen randomly from the so-called *circular unitary ensemble* (CUE). This can be achieved by the following parametrization,

$$U_i(a,b,c) = \begin{pmatrix} e^{ia}\cos(b) & e^{ic}\sin(b) \\ e^{-ic}\sin(b) & e^{-ia}\cos(b) \end{pmatrix}, \tag{5.7}$$

where a and c are uniformly sampled from $[0, 2\pi]$, and $b = \arcsin(k)$ with k uniformly in $[0, 1]$. In Cirq, we can realize Eq. (5.7) via the decomposition $U_i(a,b,c) = e^{i(a+c)Z/2} e^{ibY} e^{i(a-c)Z/2}$.

2) Once a set of U_i has been chosen, we perform repeated measurements with this given instance of random unitaries to extract the probabilities $P_U(s_A)$ of measuring a bitstring s_A of the subsystem A.
3) Finally, we repeat the above procedure many times and compute the probabilities $P_U(s_A)$ for different random operations $U = \prod_i U_i$. The second Rényi entropy of the subsystem A is then obtained from [5]

$$S^{(2)} = -\log \bar{X}, \quad \text{with } X = 2^{L_A} \sum_{s_A, s'_A} (-2)^{-D(s_A, s'_A)} P_U(s_A) P_U(s'_A), \tag{5.8}$$

where the overbar $\bar{X}$ denotes the average over different random unitaries $U = \prod_i U_i$ with the U_i chosen independently from the CUE. $D(s_A, s'_A)$ denotes the *hamming distance* between the two bitstrings s_A and s'_A, which is defined as the number of bits where the two bitstring differ, i.e. $D(s_A, s'_A) = \#\{i : s_A(i) \neq s'_A(i)\}$.

> ***Exercise 17:*** To implement the above algorithm, go through the following steps.
> **a)** Write a function U2_CUE(qubit,symbs) that returns a parametrized single-qubit operation from Eq. (5.7), applied to the qubit qubit. The symbs[0], symbs[1], symbs[2] are the parameter symbols for the values a, b, c from Eq. (5.7).
> **b)** Write a function hamming(s1,s2) that implements the above hamming distance.
> **c)** Choose around 2000 measurement repetitions for each instance of the CUE and around 200 different instances of the CUE to compute $S^{(2)}(t)$ for selected time steps between $t = 0$ and $t = 5$, again for $g = 2$ (running the algorithm with these parameters might take a while, so you can experiment with smaller values first). Use the parametrized circuits introduced in the first day of the practical. Plot and compare your result to the exact value of $S^{(2)}(t)$ from the simulated wave function.

5.5 The effects of noise

Dearling with noise in the quantum machine is in general a very tricky task and requires lots of knowledge about the device. Here, we illustrate some basic ideas of quantum error mitigation using the simplest digital error model assuming independent spin flips on each qubit, which indeed seems too simple in many real devices. But in some cases, it turns out such a simple model is found to reasonably account for the effective noise from the device, such as the device used for recent quantum supremacy paper by Google [6]. A general form of single qubit noise is realized by a quantum channel, which is a result of the interaction with the environment (from Stinespring dilation theorem). Let us consider the following form of a single-qubit depolarizing channel,

$$\rho \mapsto (1 - p_x - p_y - p_z)\rho + p_x X\rho X + p_y Y\rho Y + p_z Z\rho Z. \tag{5.9}$$

Such a channel can be simulated by sampling a wavefunction in Cirq using the same simulator as before, where Cirq will apply the Pauli errors with the specified probabilities. Note that for other, non-unitary channels we would need to use the (more costly) density matrix simulator instead.
Here, we will try to mitigate the above type of readout error by unfolding the readout matrix obtained in a calibration process before the experiment, as explained in the instructions for day 1. Let us go through the implementation in the following:

Exercise 14: First, we create a circuit that includes the noise from Eq. (5.9) in our state tomography.
a) Take a small system of 5 qubits and create a circuit 'noise' that implements the above depolarization noise using the gates

cirq.asymmetric_depolarize(px,py,pz)

which is applied to all qubits in the chain. Choose $p_x = 0.01$ and $p_y = p_z = 0.005$ for concreteness for the following tasks.
b) Simulate the time evolution up to $t = 1$ at $g = 2$ and determine the reduced density matrix of the *three rightmost qubits* from the probabilites p_{jk} that you can obtain via state tomography. However, in contrast to before, insert the circuit noise directly before performing the measurements. You can use 1000 repetitions for the tomography.
c) From the resulting reduced density matrix (use MLE_minimal(rho)!), compute the von Neumann and second Rényi entanglement entropy and compare with the result that you obtain without noise.

Exercise 15: Now, we will try to mitigate the impact of noise via the scheme introduced on the first day of the practical.
a) To perform the calibration, create a circuit that first prepares a given computational basis state $|k\rangle$ of the three qubits in the subsystem ($k = 1, ..., 2^3$), and add the depolarization noise right before measuring the three qubits. Perform repeated measurements to determine the probabilities

$$P_{lk} = \Pr\left(\text{Measured bitstring } l | \text{ Prepared bitstring } k\right) \tag{5.10}$$

for all k and l.
b) To perform the unfolding, use P_{lk} (recall that $l, k = 1, ..., 2^3$) to convert the measured, noisy probabilites p_{jk} (recall that $j = 1, ..., 3^3$; $k = 1, ..., 2^3$) that you obtained from the tomography in Exercise 14.b) into corrected probabilities $\tilde{p}_{jk}$ by inverting the relation $p_{jk} = \sum_l P_{kl}\, \tilde{p}_{jl}$ (using numpy).
c) Extract a new, error-mitigated density matrix from the probabilities $\tilde{p}_{jk}$ and compute $S(t)$ and $S^{(2)}(t)$. Compare your result with the unmitigated as well as the noise-free entanglement entropies to verify that your error-mitigation was effective.

Exercise 16: We can also investigate the impact of the above depolarization noise on the observables crucial for detecting DQPTs. Choose parameters that you deem sensible and include the noise in order to compute the Loschmidt rate for a quench across the phase transition. Compare mitigated, un-mitigated, and noise-free Loschmidt rates within a plot.

References

[1] M. Heyl, "Dynamical quantum phase transitions: a review," *Reports on Progress in Physics*, vol. 81, p. 054001, apr 2018.

[2] P. Pfeuty, "The one-dimensional Ising model with a transverse field," *Annals of Physics*, vol. 57, no. 1, pp. 79 – 90, 1970.

[3] M. G. Neeley, *Generation of Three-Qubit Entanglement Using Josephson Phase Qubits*. PhD thesis, 2010.

[4] J. A. Smolin, J. M. Gambetta, and G. Smith, "Efficient Method for Computing the Maximum-Likelihood Quantum State from Measurements with Additive Gaussian Noise," *Phys. Rev. Lett.*, vol. 108, p. 070502, Feb 2012.

[5] A. Elben, B. Vermersch, C. F. Roos, and P. Zoller, "Statistical correlations between locally randomized measurements: A toolbox for probing entanglement in many-body quantum states," *Phys. Rev. A*, vol. 99, p. 052323, May 2019.

[6] F. Arute, K. Arya, R. Babbush, *et al.*, "Quantum supremacy using a programmable superconducting processor," *Nature*, vol. 574, no. 7779, pp. 505–510, 2019.